

Smelting in the age of nano: iron aerogels

Nicholas Leventis,*^a Naveen Chandrasekaran,^a Chariklia Sotiriou-Leventis,^a and Arif Mumtaz^b

^a Department of Chemistry, Missouri University of Science & Technology, Rolla, MO 65409, U.S.A. Fax: 573-341-6033; Tel: 573-341-4391; E-mail: leventis@mst.edu

^b Department of Physics, Quaid-i-Azam University, Islamabad, Pakistan. Tel: +92-51-96042127; E-mail: arif@qau.edu.pk

Electronic Supplementary Information

1. Photographs of native (n-) and crosslinked (X-) resorcinol-formaldehyde/iron oxide aerogels before (n-RF-FeOx, X-RF-FeOx), and after pyrolysis at 1000 °C under Ar (n-C-Fe and X-C-Fe)
2. pH changes during gelation at 80 °C of:
 $[Fe(H_2O)_6]^{3+}/CH_3CN:EtOH$ (1:1 v/v)/epichlorohydrine;
 $[Fe(H_2O)_6]^{3+}/CH_3CN: EtOH$ (1:1 v/v)/RF; and,
 $[Fe(H_2O)_6]^{3+}/CH_3CN: EtOH$ (1:1 v/v)/RF/epichlorohydrine
3. Photographs of the:
 $[Hf(H_2O)_6]^{4+}/CH_3CN: EtOH$ (1:1 v/v)/RF/epichlorohydrine (A); and, the
 $[Fe(H_2O)_6]^{3+}/CH_3CN: EtOH$ (1:1 v/v)/RF/epichlorohydrine (B) system during gelation
4. TGA data for n-RF-FeOx and X-RF-FeOx
5. Typical EDS data for n-RF-FeOx and X-RF-FeOx aerogels
6. XRD experimental and data for n-RF-FeOx aerogels as a function of the pyrolysis temperature
7. N₂ sorption isotherms for n-RF-FeOx, X-RF-FeOx, n-C-Fe and X-C-Fe
8. Temperature dependence of the zero-field-cooled magnetization for the X-C-Fe sample produced by pyrolysis of X-RF-FeOx at 800 °C under Ar.

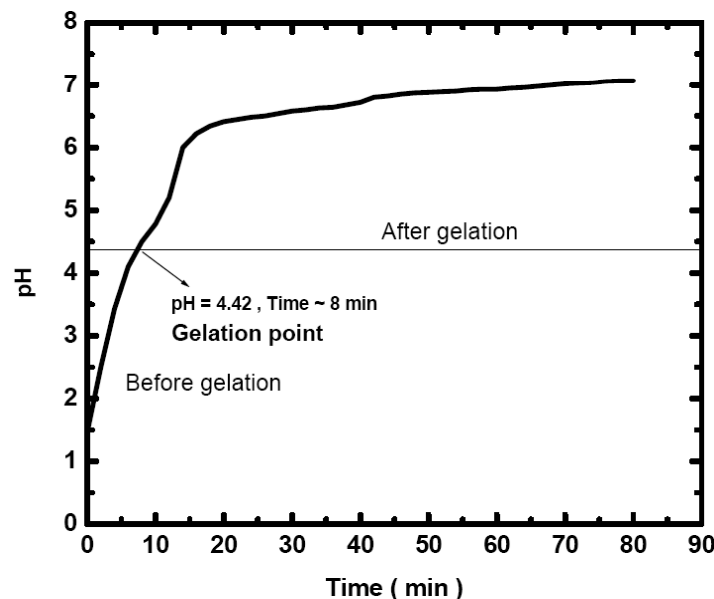
1. Photographs of native (n-) and crosslinked (X-) resorcinol-formaldehyde/iron oxide aerogels before (n-RF-FeOx, X-RF-FeOx), and after pyrolysis at 1000 °C under Ar (n-C-Fe and X-C-Fe)



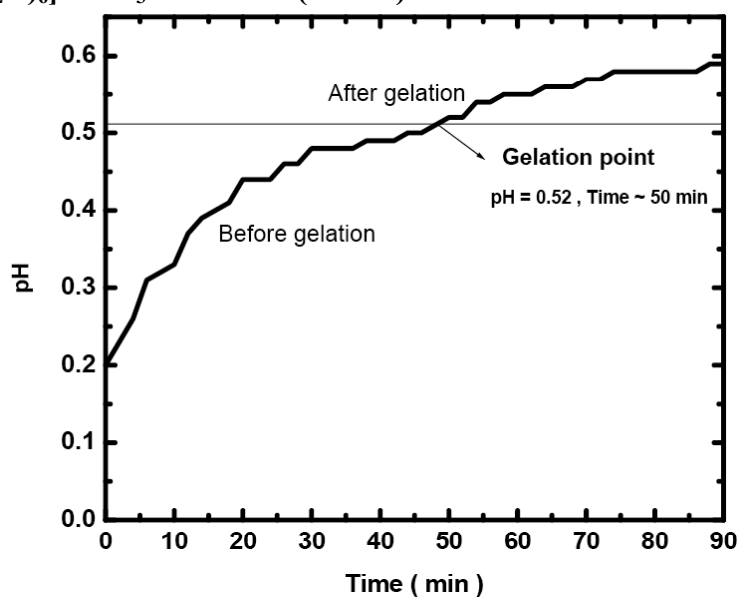
- a. n-RF-FeOx aerogel as prepared
- b. X-RF-FeOx aerogel as prepared
- c. n-C-Fe by pyrolysis of a n-RF-FeOx aerogel at 1000 °C under Ar
- d. X-C-Fe by pyrolysis of a X-RF-FeOx aerogel at 1000 °C under Ar

After pyrolysis at 1000 °C under Ar, n-RF-FeOx breaks up in large chunks. After pyrolysis under similar conditions, X-RF-FeOx remains a monolith.

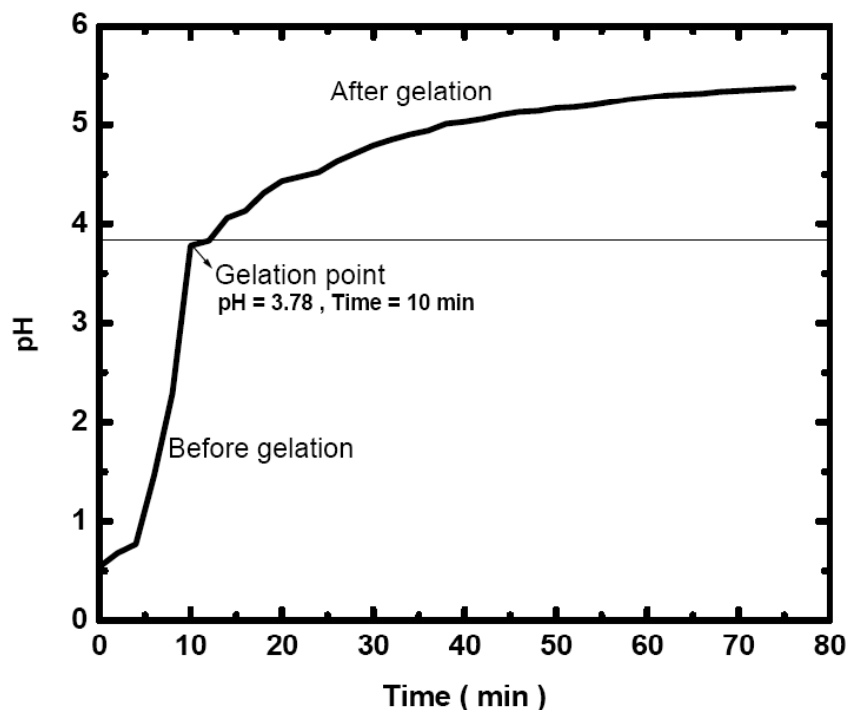
2. pH changes during gelation at 80 °C of:
 $[\text{Fe}(\text{H}_2\text{O})_6]^{3+}/\text{CH}_3\text{CN}:\text{EtOH}$ (1:1 v/v)/epichlorohydrine



pH changes during gelation at 80 °C of:
 $[\text{Fe}(\text{H}_2\text{O})_6]^{3+}/\text{CH}_3\text{CN}:\text{EtOH}$ (1:1 v/v)/RF

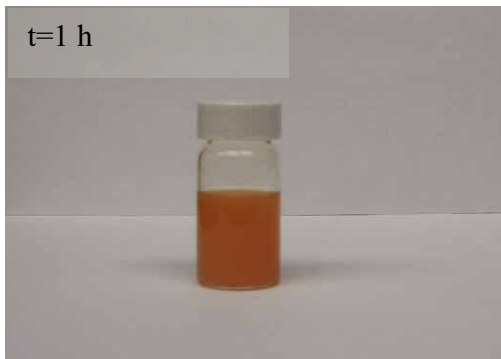
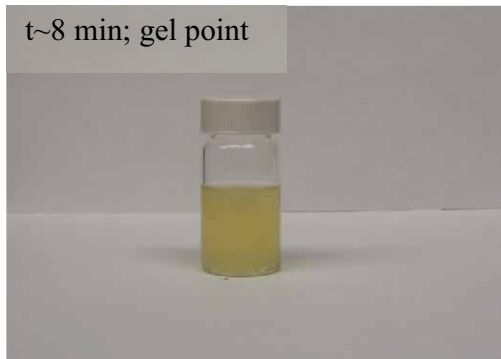


**pH changes during gelation at 80 °C of:
[Fe(H₂O)₆]³⁺/CH₃CN: EtOH (1:1 v/v)/RF/epichlorohydrine**

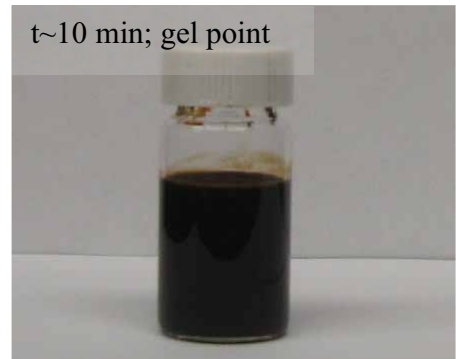


**3. Photographs of the:
[Hf(H₂O)₆]⁴⁺/CH₃CN: EtOH (1:1 v/v)/RF/epichlorohydrine (A); and, the
[Fe(H₂O)₆]³⁺/CH₃CN: EtOH (1:1 v/v)/RF/epichlorohydrine (B) system during
gelation**

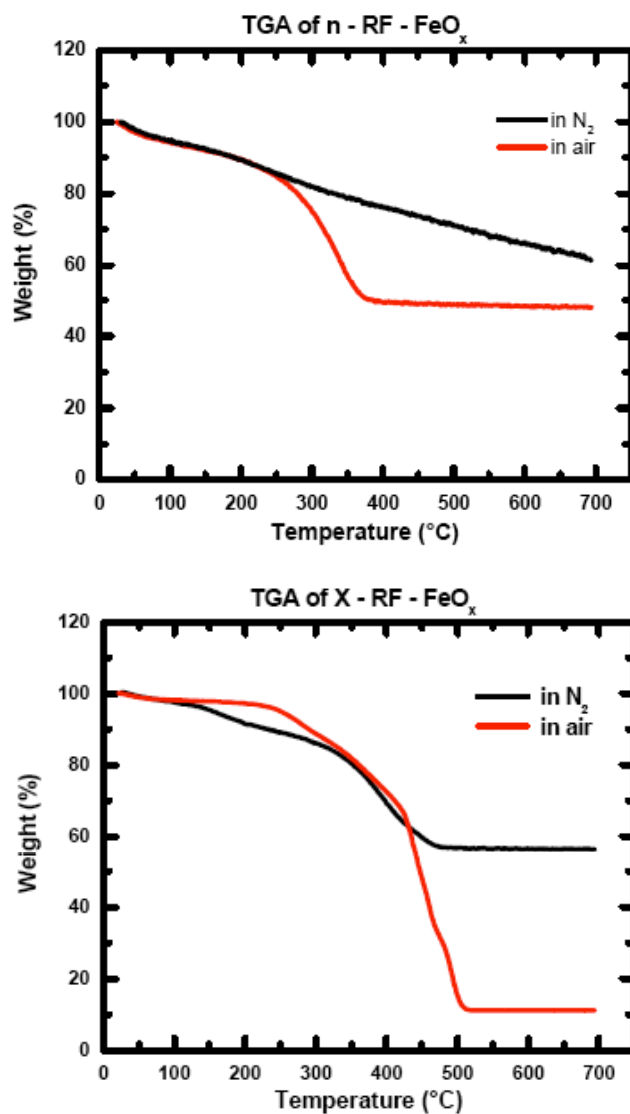
A.



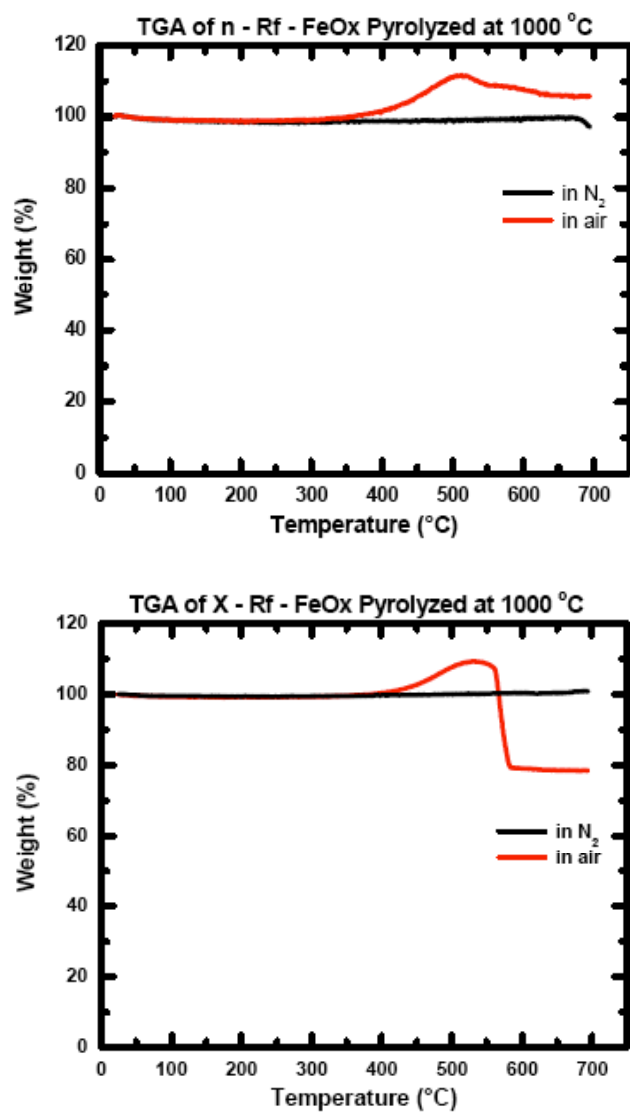
B.



4. TGA data for n-RF-FeO_x and X-RF-FeO_x



Control TGA experiments involving analysis of pyrolyzed samples

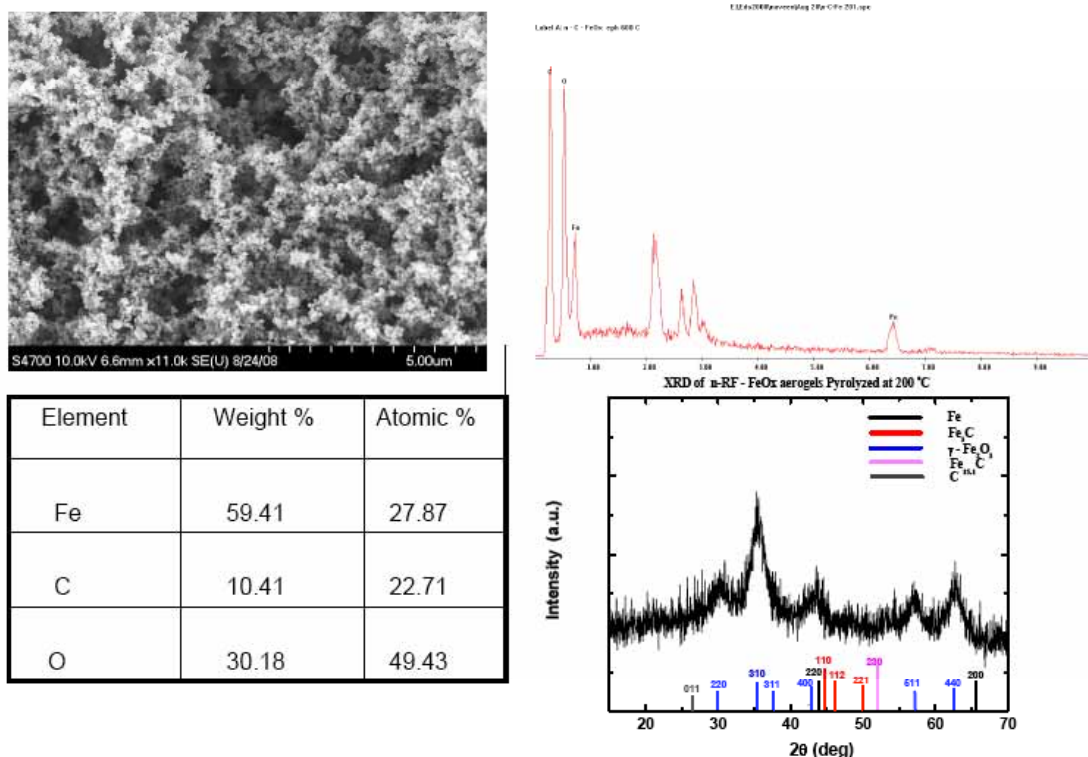


The mass increase in air is due to conversion of Fe to Fe₂O₃.

5. Typical EDS data for n-RF-FeOx and X-RF-FeOx aerogels

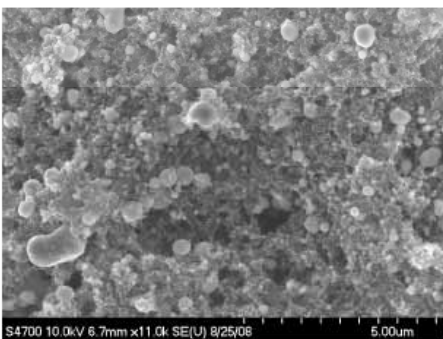
Scanning electron microscopy (SEM) and energy-dispersive x-ray spectroscopy (EDS) were conducted with a Hitachi S-4700 field emission microscope. RF-FeO_x aerogel samples for SEM were sputter-coated with Au/Pd for 2 min to avoid charging; that treatment was not necessary for iron aerogels, because they were electrically conducting.

n-RF-FeO_x aerogel pyrolyzed at 200 °C under Ar

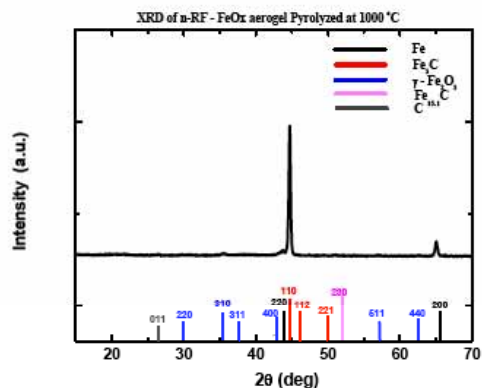
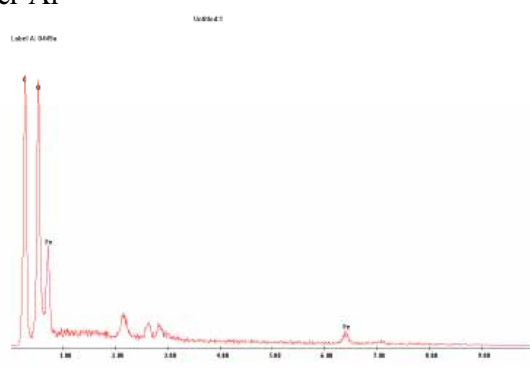


(Unlabeled peaks in the EDAX spectrum correspond to Au-Pd evaporated on the sample in order to avoid charging.)

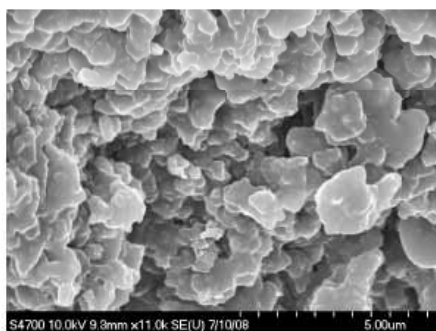
n-RF-FeOx aerogel pyrolyzed at 1000 °C under Ar



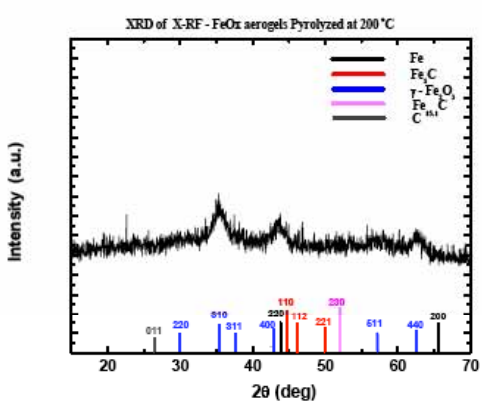
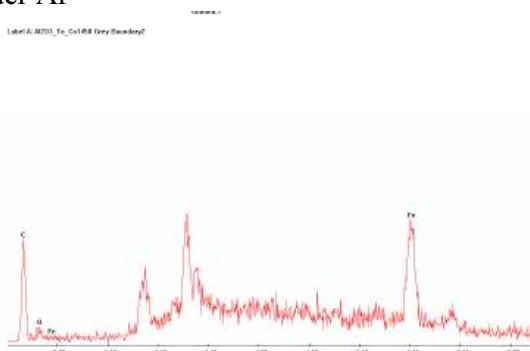
Element	Weight %	Atomic %
Fe	95.10	80.66
C	4.90	19.34
O	0.00	0.00



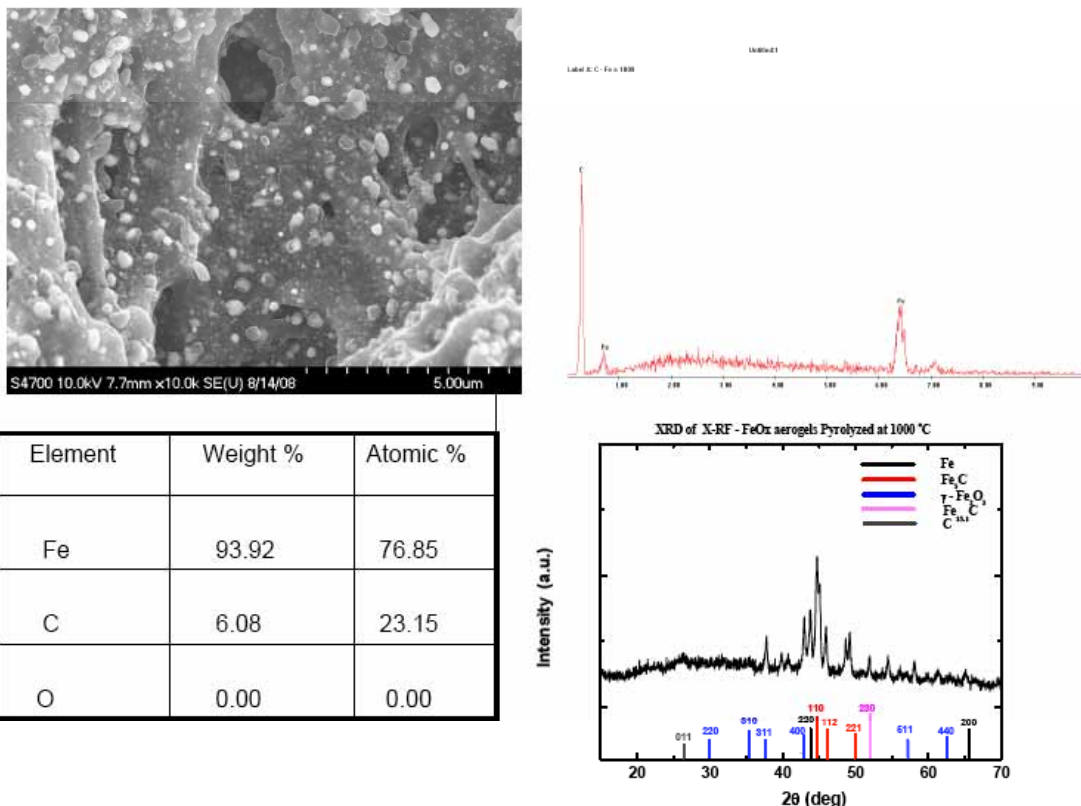
X-RF-FeOx aerogel pyrolyzed at 200 °C under Ar



Element	Weight %	Atomic %
Fe	48.00	21.0
C	24.10	46.00
O	27.9	33.00



X-RF-FeOx aerogel pyrolyzed at 1000 °C under Ar



(Since the sample was electrically conducting itself, it was not coated with Au-Pd.)

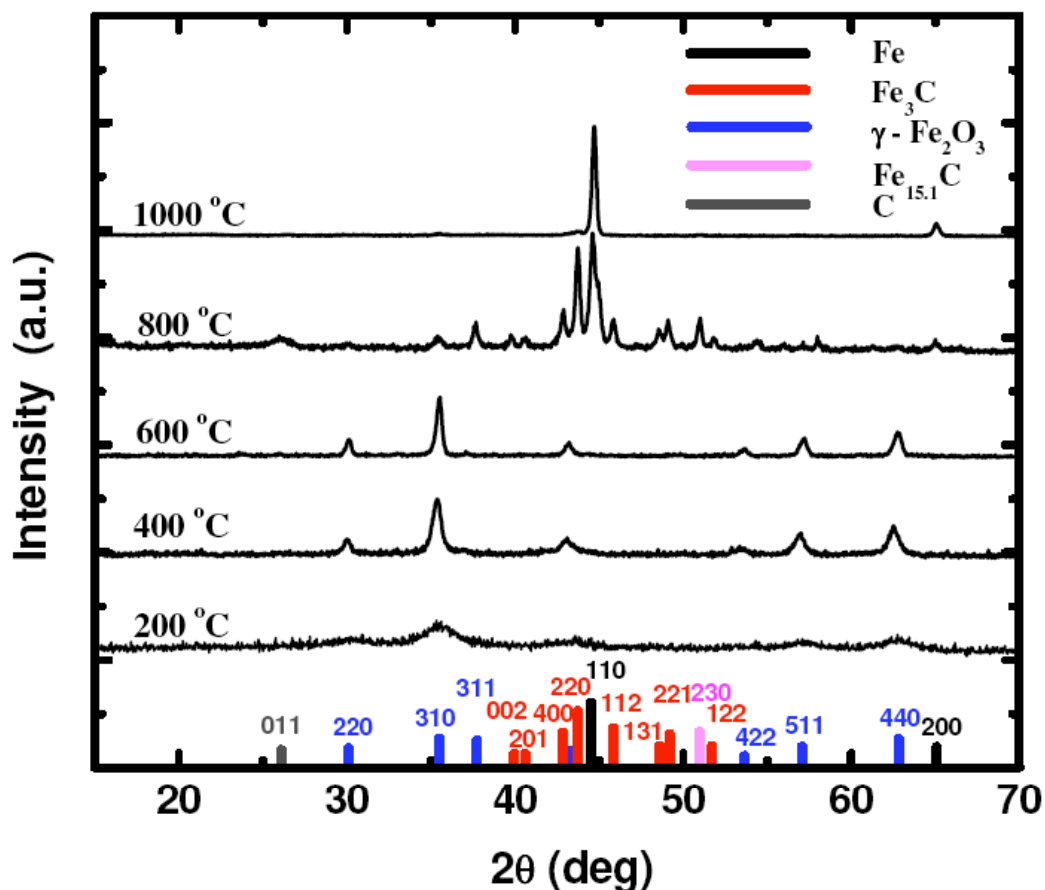
6. XRD experimental and data for n-RF-FeOx aerogels as a function of the pyrolysis temperature

Experimental details for XRD:

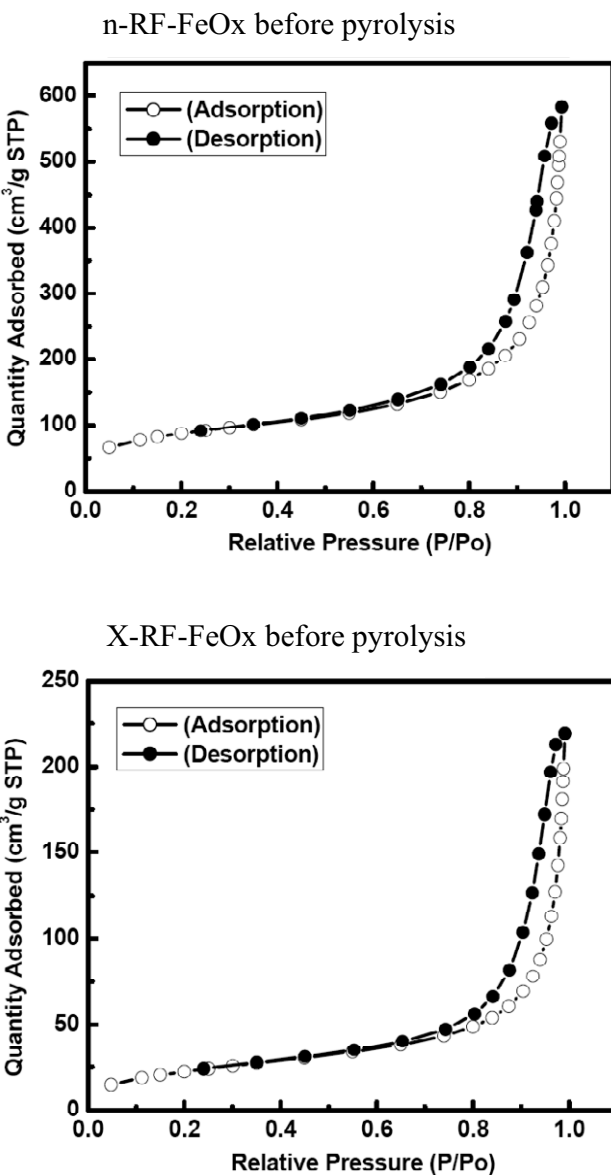
X ray diffraction experiments were performed with powders of the corresponding materials with a Scintag 2000 diffractometer using Cu K α radiation. The detector used was a proportional counter detector equipped with a flat graphite monochromator.

Quantitative analysis and Particle size analysis:

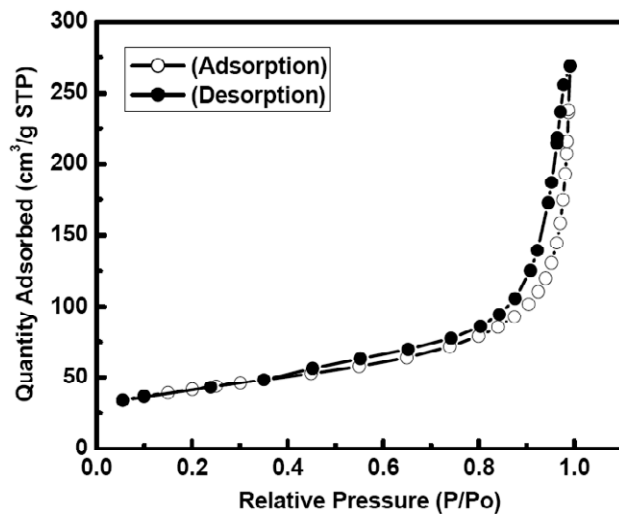
Phase composition was estimated via Rietveld refinement of the x-ray diffraction patterns utilizing RIQAS software (Materials Data, Inc., version 4.0.0.26). Structural information for each phase was obtained from the ICSD database version 2.01. Particle size was estimated using Jade software (version 5.0, Materials Data, Inc.). A Gaussian correction for instrumental broadening was applied utilizing NIST SRM 660a LaB6 to determine the instrumental broadening.



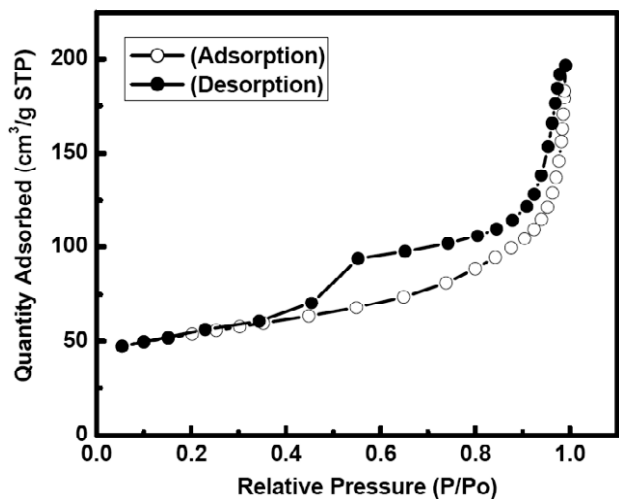
7. N₂ sorption isotherms for n-RF-FeOx, X-RF-FeOx, n-C-Fe and X-C-Fe



n-RF-FeOx after pyrolysis at 800 °C under Ar



X-RF-FeOx after pyrolysis at 800 °C under Ar



8. Temperature dependence of the zero-field-cooled magnetization for the X-C-Fe sample produced by pyrolysis of X-RF-FeOx at 800 °C under Ar

(Data were recorded while the sample was warmed in a 100 Oe field.)

The temperature dependence of the magnetization in the case of zero field cooling shows a peak at around 140K that may be attributed to the blocking temperature.

